Environmental Science
Water Research & Technology

Integrated Shortcut Nitrogen and Biological Phosphorus Removal from Mainstream Wastewater: Process Operation and Modeling

Journal:	*Environmental Science: Water Research & Technology*
Manuscript ID	EW-ART-06-2019-000550.R1
Article Type:	Paper

SCHOLARONE™
Manuscripts

Water Impact Statement:

Surface water eutrophication from excess limiting nutrients is a growing environmental problem worldwide. Nitrogen and phosphorus removal from wastewater is a critical part of the solution, but often requires added chemicals and energy due to aeration. This study demonstrates combined nitrogen and phosphorus removal from real wastewater without added chemicals, and nitrogen removal is achieved through the energy-saving nitritation-denitritation process.

Integrated Shortcut Nitrogen and Biological Phosphorus Removal from Mainstream Wastewater: Process Operation and Modeling

Paul Roots[a], Fabrizio Sabba[a], Alex F. Rosenthal[b], Yubo Wang[a], Quan Yuan[c], Leiv Rieger[b], Fenghua Yang[d], Joseph A. Kozak[d], Heng Zhang[d], George F. Wells[a*]

[a]Department of Civil and Environmental Engineering, Northwestern University, 2145 Sheridan Road, Evanston, IL, 60208, USA

[b]inCTRL Solutions, Inc., Dundas, Ontario, Canada

[c]Tsinghua University, Haidian District, Beijing, China

[d]Metropolitan Water Reclamation District of Greater Chicago, 6001 W Pershing Road, Chicago, IL, 60804, USA

[*]Corresponding Author: George Wells. Phone: (847) 491-8794. Email: george.wells@northwestern.edu

Abstract

While enhanced biological phosphorus removal (EBPR) is widely utilized for phosphorus (P) removal from wastewater, understanding of efficient process alternatives that allow combined biological P removal and shortcut nitrogen (N) removal, such as nitritation-denitritation, is limited. Here, we demonstrate efficient and reliable combined total N, P, and chemical oxygen demand removal (70%, 83%, and 81%, respectively) in a sequencing batch reactor (SBR) treating real mainstream wastewater (primary effluent) at 20°C. Anaerobic – aerobic cycling (with intermittent oxic/anoxic periods during aeration) was used to achieve consistent removal rates, nitrite oxidizing organism (NOO) suppression, and high effluent quality. Importantly, high resolution process monitoring coupled to *ex situ* batch activity assays demonstrated that robust biological P removal was coupled to energy and carbon efficient nitritation-denitritation, not simultaneous nitrification-denitrification, for the last >400 days of 531 total days of operation. Nitrous oxide emissions of 2.2% relative to the influent TKN (or 5.2% relative to total inorganic nitrogen removal) were similar to those measured in other shortcut N bioprocesses. No exogenous chemicals were needed to achieve consistent process stability and high removal rates in the face of frequent wet weather flows and highly variable influent concentrations. Process modeling reproduced the performance observed in the SBR and confirmed that nitrite drawdown via denitritation contributed to suppression of NOO activity.

Keywords

Nitritation-denitritation, enhanced biological phosphorus removal (EBPR), polyphosphate accumulating organisms (PAO), biological nutrient removal (BNR), NOO out-competition, nitrite oxidizing bacteria (NOB)

1. Introduction

Nitrogen (N) and phosphorus (P) are key limiting nutrients in surface waters, and their removal from wastewater is becoming increasingly important due to widespread eutrophication in both marine and lacustrine environments. While denitrification with exogenous carbon addition to remove N as well as chemical precipitation to remove P are well-established methods to meet nutrient discharge limits, utilities are seeking more efficient and cost-effective methods to meet their permits. Enhanced biological P removal (EBPR) is increasingly implemented as an economical alternative to chemical P precipitation, and emerging innovations in shortcut N removal processes, including nitritation coupled to heterotrophic denitritation via out-competition of nitrite oxidizing organisms (NOO)[1], offer a route to low-energy, low-carbon biological N removal[2]. However, the drivers that select for NOO out-competition in shortcut N removal processes and their impact on biological P removal are little understood.

While several studies have proposed 2-stage systems with separate sludge for N and P removal from mainstream wastewater[3–7], single sludge systems simplify operations and maintenance and can reduce both capital and ongoing costs over 2-stage systems. A limited number of lab-scale studies have used single-sludge systems to incorporate shortcut N removal with P removal from synthetic wastewater feed[8–10]. Given that chemical oxygen demand (COD) can be limiting in nutrient removal systems, it is important to note that all three of the referenced studies used readily biodegradable acetate in the synthetic feed as their primary carbon source in 10:1 g acetate-COD:gN and 27:1 g acetate-COD:gP ratios or higher. While promising proof of concepts, use of synthetic feed at such high VFA:N and VFA:P ratios is not representative of the dynamics in N, P, and COD composition commonly found in real wastewater.

Investigations of combined shortcut N and P removal from real wastewater without exogenous carbon or chemical addition for P precipitation are limited to two lab-scale reactors[11,12] and two full scale processes[13,14], but one of the lab-scale and both full scale processes had average wastewater temperatures between 26 and 30 °C. Such elevated temperatures confer a significant advantage to ammonia oxidizing organisms (AOO, which can include both ammonia oxidizing bacteria and archaea) over NOO, thereby greatly facilitating NOO out-competition[15], but are not representative of conditions found in WWTPs in temperate regions. In the lab-scale reactor with high temperature cited above, for instance, Zeng et al. (2014)[11] lost NOO out-selection when the wastewater temperature dropped below 23 °C as winter approached. The other lab-scale process was operated at a more moderate temperature range of 18 – 26 °C, but was hampered by long hydraulic retention times (HRT) of 17.5 – 55 hours due to its reliance on post endogenous denitrification for N removal[12,16]. Research into combined shortcut N and EBPR processes with real wastewater at moderate temperatures (i.e. ≤ 20 °C), where NOO suppression is significantly more challenging[17], is currently lacking. Intermittent aeration is one promising strategy for NOO suppression at moderate temperatures. Explanations for its efficacy range from a metabolic lag phase of *Nitrospira* NOO compared to AOO upon exposure to oxygen[18] to transient exposure to free ammonia due to pH shifts in biofilms[19], as free ammonia has a greater inhibitory effect on NOO than AOO[20,21]. However, the mechanism and efficacy of intermittent aeration for NOO suppression at moderate temperatures, with or without integration of biological P removal, is currently not well understood.

Process modeling of combined shortcut N and P removal systems is very limited due to the novelty of such systems; none of the above-cited studies included whole-system models. Some modeling efforts to date have focused on NOB out-competition in shortcut N systems[22–24], but

integration with biological phosphorus removal is limited. Of interest in the present study is whether a commercially available modeling platform can replicate observed nutrient dynamics in an integrated shortcut N and P removal process, and thus providing a valuable tool for insight and interpretation.

The propensity for shortcut N removal systems to produce nitrous oxide (N_2O), a potent greenhouse gas, is little understood, though reports suggest that N_2O production may exceed that of conventional N removal biotechnologies[25–28]. For example, in one of the lab scale studies cited above, Zeng et al. (2003)[10], N_2O production exceeded N_2 production from a lab-scale nitritation-denitritation process by more than 3-fold. However, none of the above studies using real wastewater[11,13,14] measured N_2O emissions. Therefore, N_2O measurements on shortcut N removal systems integrated with biological P removal from real wastewater are of interest to accurately assess their net impact on greenhouse gas emissions.

Here, we demonstrate efficient and reliable combined shortcut N, P, and COD removal in a sequencing batch reactor (SBR) treating real mainstream wastewater (primary effluent) at 20°C. In contrast to the synthetic studies cited above, the primary effluent used here as influent contained average ratios of 1:1 gVFA-COD:gTKN and 8.2:1 gVFA-COD:gTP, comprising a challenging environment for total nutrient removal. Importantly, EBPR was coupled to nitritation-denitritation for energy and carbon-efficient N removal. A simple kinetic explanation for the out-competition of NOO via intermittent aeration and SRT control was illustrated via batch tests and process modeling. No exogenous chemicals were needed to achieve consistent process stability and high removal rates in the face of frequent rain events and highly variable influent concentrations.

2. Materials and Methods

2.1 Reactor inoculation and operation

A 56-L reactor was seeded with activated sludge biomass from another pilot EBPR bioreactor (grown on the same wastewater) on June 15, 2017 (day 0 of reactor operation) and fed primary settling effluent from the Terrance J. O'Brien WRP in Skokie, IL for 531 days. Online sensors included the ammo::lyser™ eco+pH ion-selective electrode for $NH_4^+$and pH, the oxi::lyser™ optical probe for dissolved oxygen (DO), and the redo::lyser™ eco potentiometric probe for oxidation-reduction potential (ORP) (s::can, Vienna, Austria). The reactor was operated with code-based Programmable Logic Control (PLC) (Ignition SCADA software by Inductive Automation, Fulsom, CA, USA, and TwinCAT PLC software by Beckhoff, Verl, Germany) as a sequencing batch reactor (SBR) with cycle times detailed in Table 1. An anaerobic react period followed by an intermittently aerated period was chosen with the intent to select for integrated biological P removal and nitritation/denitritation via suppression of NOO activity. The reactor was temperature-controlled to target 20°C (actual temperature = 19.8 ± 1.0°C) via a heat exchange loop to evaluate performance at moderate temperatures. The pH was not controlled and varied between 7.0 and 7.8.

The variable-length aerated react period was terminated if either a maximum allowable react time was reached (usually between 300 – 480 minutes) or if the target NH_4^+ concentration was reached according to the online sensor. Intermittent aeration was used during the aerated react period with the following loop:

1. 4 or 5 minutes of aeration with proportional-integral (PI) control to target 1 mgO_2/L via the online DO probe. PI control managed the percent-open time of an air solenoid

valve, which, when open, provided compressed air at 7 – 15 liters per minute through a 5-inch diameter aquarium stone disk diffusor at the bottom of the reactor. (Compressed air was provided via a California Air Tools model 5510SE air compressor [San Diego, CA, USA]. The 7 – 15 LPM flow rate was selected based on expected oxygen demand and modified to allow for rapid realization of the 1 mgO_2/L target DO level.)

2. After aeration, shut air solenoid valve and wait until DO drops to < 0.05 mgO_2/L.
3. Run "anoxic" timer for 0 – 3 minutes. At end of timer, return to Step 1.

Due to variable oxygen uptake rates (OUR) and changes to the anoxic timer, the overall aerobic/anoxic interval lengths typically varied between 10 – 20 minutes. Because react length varied with influent NH_4^+ concentration (due to NH_4^+ sensor-based control), the SBR loading rate followed that of the full-scale plant, i.e. with shortened SBR cycles and increased flow during wet-weather events.

The process timeline is split into 2 phases to simplify reporting: Phase 1 (days 0 - 246) and Phase 2 (days 247 – 531), the latter of which represents lower target effluent N concentrations (1.5 – 2 $mgNH_4^+$-N/L, vs. 3 – 5 $mgNH_4^+$-N/L during Phase 1) and better N-removal performance. Phase 1 was used as a process optimization period to determine the optimal SRT for NOO washout with AOO retention.

SRT was controlled via timed mixed liquor wasting after the aerated react phase, and solids losses in the effluent were included in the dynamic SRT calculation, following the methodology of [24]. Using an operational definition of "aerobic" as > 0.2 mgO_2/L, an analysis of 4 cycles from Phase 2 showed that an average 48% of the time within the intermittently aerated react period is aerobic. See the Supporting Information for details regarding SRT control and calculations.

Composite sampling as summarized in Table S1 was initiated on day 27 after an initialization period to allow the accumulation of AOO as measured by ammonia oxidation activity. Beginning on day 114 and to the end of the study, influent COD fractionation analysis was conducted once per week with the following definitions [29]:

- Particulate COD = Total COD – 1.2-µm filtered COD
- Colloidal COD = 1.2-µm filtered COD – floc-filtered COD
- Soluble COD (not including VFAs) = floc-filtered COD – VFA
- VFA COD = VFA

Floc-filtered COD was measured as described in Mamais et al. (1993) and total COD, filtered COD and VFAs were analyzed per Standard Methods [31]. On average, the total COD and VFA to nutrient ratios of the influent were (Table S2):

- 8.3:1 g total COD:g TKN
- 1:1 g VFA-COD:g TKN
- 67:1 g totalCOD:g totalP
- 8.2:1 g VFA-COD:g totalP

2.2 Batch activity assays

2.2.1 In-cycle batch activity assays

Seventeen in-cycle batch activity assays were conducted throughout the study to monitor *in situ* dynamics of NH_4^+, NO_2^-, NO_3^-, PO_4^{3-} (all tests), readily biodegradable COD (rbCOD - two tests) and volatile fatty acids (VFAs – one test) via Standard Methods[31] and Mamais et al. (1993)[30] for rbCOD. Samples were taken every 15 – 45 minutes for a full SBR cycle, except in the case of two high-frequency tests, in which samples were taken every one to two minutes for 40 minutes in the aerated portion of the cycle to investigate high time resolution nutrient dynamics during intermittent aeration.

2.2.2 *Ex situ* batch activity assays

176 *Ex situ* maximum batch activity assays for AOO and NOO were performed as previously
177 described[32,33]. *Ex situ* activity assays were also employed to quantify biological P uptake of
178 polyphosphate accumulating organisms (PAOs) under aerobic and denitrifying conditions.
179 Relative P-uptake rates via different electron acceptors under typical in-reactor conditions was
180 desired (as opposed to maximum P-uptake rates), so external carbon was not added. 250-mL
181 aliquots of mixed liquor were removed from the reactor following the anaerobic phase (i.e. after P
182 release and VFA uptake) and placed in air-tight 250-mL serum bottles. The sealed bottles were
183 injected with sodium nitrite or potassium nitrate stock solutions to approximately 9 mgN/L of NO_2^-
184 or NO_3^- for the anoxic (denitrifying) uptake tests or opened and bubbled with air through an
185 aquarium diffusor stone for aerobic tests. A replicate for the aerobic test was provided by the 56-
186 L reactor itself, which was also aerated continuously (with a resulting DO concentration of 2 mg/L)
187 and sampled in parallel with the aerated serum bottle. A control assay utilized biomass with no
188 electron acceptors (O_2, NO_3^-, or NO_2^-) provided. Serum bottles were mixed by a Thermo Scientific
189 MaxQ 2000 shaker table (Waltham, MA) at 150 RPM and at ambient temperature near 20°C. P
190 uptake was quantified via a least squares regression of the PO_4^{3-} measurement from 3 – 5 samples
191 taken every 20 minutes and normalized to the reactor VSS. The results represent the average ±
192 standard deviation of three total replicates for each electron acceptor from days 237 and 286.

193

194 **2.2.3 In-cycle batch activity assays for quantification of N_2O emissions**

195 N_2O emissions from the reactor were estimated during Phase 2 by measuring the aqueous N_2O
196 concentration over 8 separate cycles from days 414 to 531 with a Unisense N_2O Wastewater Sensor
197 equipped with the E-N_2O Head with a working range of 0 – 1.5 mg N_2O-N/L (Aarhus, Denmark).
198 N_2O emissions were calculated from the aqueous concentration following Domingo-Félez et al.
199 (2014), after measuring the N_2O stripping rate during aeration with mixing and during mixing

alone. NH_4^+, NO_2^- and NO_3^- were measured concurrently at the beginning and end of cycles[31] to calculate TIN removal. N_2O emissions were then quantified relative to TIN removal and the TKN load for each of the eight cycles.

2.3 Process Modeling

To evaluate mechanisms of NOO suppression and the balance between aerobic PAO and denitrifying PAO (DPAO) activity, the SIMBA#3.0.0 wastewater process modeling software (ifak technology + service, Karlsruhe, Germany) was used to simulate performance of the reactor during Phase 2 of operation. We utilized the inCTRL activated sludge model (ASM)[34,35], an established engineering model applied extensively in the field and which is based on Barker and Dold (1997)[36]with the addition of two-step nitrification-denitrification, methanotrophs, and other extensions (see Supporting Information for the entire inCTRL ASM matrix, fractions, parameters and variables). The objective of modeling was to see if an established engineering model could predict observed behavior without adjustment of kinetic or stoichiometric parameters, and thus provide insight into the operation and optimization of the modeled reactor. Default Monod half-saturation constants of particular relevance to this study include oxygen affinity of AOO ($K_{O2,AOO} = 0.25$ mgO_2/L) and NOO ($K_{O2,NOO} = 0.15$ mgO_2/L), substrate affinity of AOO ($K_{NHx,AOO} = 0.7$ mgNH_X-N/L; NH_X = NH_4^+ + NH_3) and NOO ($K_{NO2,NOO} = 0.1$ mgNO_2^--N/L), and maximum specific growth rate of AOO (μ_{AOO} = 0.9 d^{-1}) and NOO (μ_{AOO} = 0.7 d^{-1}). All default values listed above from the inCTRL ASM were intentionally left unmodified, but due to their importance in modeling nitrite-shunt systems, a brief discussion is in order. The commonly used parameter values from Wiesmann (1994)[37] suggest a higher oxygen and substrate affinity of *Nitrosomonas*

AOO than *Nitrobacter* NOO, but more recent measurements demonstrate the high NO_2^- affinity ($K_{NO2,NOO}$ = 0.1 – 0.4 mgNO_2-N/L[38]) and oxygen affinity ($K_{O2,NOO}$ = 0.09 mgO_2/L[39]) of *Nitrospira* NOO (*Nitrospira* were found in this study via 16S rRNA gene sequencing, along with *Nitrotoga* NOO). More recent measurements of *Nitrosomonas* AOO (also found in this study) substrate and oxygen affinity[40] confirm those measured by Wiesmann[37] and are similar to those used here. The implications of higher substrate and oxygen affinities for NOO than AOO is that modeled NOO out-competition will be relatively more difficult to achieve. The exception to this AOO advantage is the slightly higher modeled maximum specific growth rate of AOO over NOO, though this is supported by Law et al. (2019)[39], wherein *Nitrosomonas* AOO were shown to have a much higher maximum specific growth rate than *Nitrospira* NOO.

SBR control of the reactor was simulated directly using a petri net approach, with sequence control shown as green blocks in Figure S1. To avoid rounding errors and to improve simulation speed, the reactor was modeled with a 56 m^3 working volume as opposed to 56 L. As in the reactor, the modeled anoxic period was fixed at 45 minutes and the aerobic period ended when soluble NH_X (i.e. NH_4^+ + NH_3, which is approximately equal to NH_4^+ at the pH values encountered of 7.0 – 7.8) was < 2 mgN/L. Modeled intermittent aeration during the aerobic period was controlled as described in the Supporting Information, though a slightly longer "anoxic" timer of 3 min 45 seconds in the model was used (vs. 0 – 3 minutes in the actual SBR) to account for the DO sensor delay in the actual SBR. Modeled mixed liquor wasting was adjusted until the calculated model SRT (which included effluent solids) matched the SRT of the reactor during Phase 2. 5/8 volume decant was performed at the end of the cycle and average primary effluent (reactor influent) values from Phase 2 were used as model influent. The initialization procedure involved running the model for 150 days to achieve quasi steady-state conditions. Modeled specific growth rates for AOO,

NOO, and PAOs were quantified throughout the SBR cycles with rate equations and parameter values from the SIMBA# inCTRL ASM matrix.

$$\mu_{AOO} = net\ specific\ growth\ rate\ of\ AOO\ (d^{-1})$$
$$\mu_{NOO} = net\ specific\ growth\ rate\ of\ NOO\ (d^{-1})$$

The washout SRT for NOO was calculated from μ_{NOO} as detailed in the Supporting Information.

Modeled PAO growth rates as discussed in this paper include growth on PHA associated with P uptake but do not include decay or PAO growth on PHA where PO_4^{3-} is limiting. Also, the SIMBA# inCTRL ASM matrix considers only a single PAO population with an anoxic growth factor ($\eta_{anox,PAO} = 0.33$) in the DPAO rate equations to estimate anoxic P uptake (see Supporting Information for full rate equations). The three growth rates below therefore represent growth of a single functional group split between 3 electron acceptors: O_2, NO_2^-, and NO_3^-.

$$\mu_{PAO,O2} = PAO\ growth\ associated\ with\ O_2\ (d^{-1})$$
$$\mu_{PAO,NO2} = PAO\ growth\ associated\ with\ NO_2^-\ (d^{-1})$$
$$\mu_{PAO,NO3} = PAO\ growth\ associated\ with\ NO_3^-\ (d^{-1})$$

Rate equations and parameters values for the above modeled growth rates, along with the process representation in SIMBA#, can be found in the Supporting Information.

2.4 Biomass sampling and DNA extraction

Reactor biomass was archived biweekly for sequencing-based analyses. Six 1 mL aliquots of mixed liquor were centrifuged at 10,000g for 3 minutes, and the supernatant was replaced with 1 mL of tris-EDTA buffer. The biomass pellet was then vortexed and centrifuged at 10,000g for 3 minutes after which the supernatant was removed, leaving only the biomass pellet to be transferred

to the -80°C freezer. All samples were kept at -80°C until DNA extraction was performed with the FastDNA SPIN Kit for Soil (MPBio, Santa Ana, CA, USA) per the manufacturer's instructions.

2.5 16S rRNA gene amplicon sequencing

16S rRNA gene amplicon library preparations were performed using a two-step multiplex PCR protocol, as previously described [41]. All PCR reactions were performed using a Biorad T-100 Thermocycler (Bio-Rad, Hercules, CA). The V4-V5 region of the universal 16S rRNA gene was amplified in duplicate from 20 dates collected over the course of reactor operation using the 515F-Y/926R primer set [42]. Further details on thermocycling conditions, reagents, and primer sequences can be found in Supporting Information.

All amplicons were sequenced using a MiSeq system (Illumina, San Diego, CA, USA) with Illumina V2 (2x250 paired end) chemistry at the University of Illinois at Chicago DNA Services Facility and deposited in GenBank (accession number for raw data: PRJNA527917). Procedures for sequence analysis and phylogenetic inference can be found in the Supporting Information.

2.6 Quantitative Polymerase Chain Reaction (qPCR)

qPCR assays were performed targeting the ammonia oxidizing bacterial *amoA* gene via the *amoA*-1F and *amoA*-2R primer set [43], and total bacterial (universal) 16S rRNA genes via the Eub519/Univ907 primer set [44]. All assays employed thermocycling conditions reported in the reference papers and were performed on a Bio-Rad C1000 CFX96 Real-Time PCR system (Bio-Rad, Hercules, CA, USA). Details on reaction volumes and reagents can be found in the Supporting Information. After each qPCR assay, the specificity of the amplification was verified with melt curve analysis and agarose gel electrophoresis.

3. Results and Discussion

3.1 Nitrogen, AOO and NOO

3.1.1 Overall Performance and Nitrogen Removal

To demonstrate feasibility and evaluate optimal operational conditions for integrated biological P and shortcut N removal via NOO out-selection at moderate temperatures, we operated lab-scale reactor fed with real primary effluent for 531 days. Reactor operation proceeded in two phases. Reactor performance across both phases is shown in Figure 1 and summarized in Table 2. Phase 1 (days 0-246) established proof-of-concept for the compatibility of N removal via nitritation-denitritation via intermittent aeration with EPBR and allowed for optimization of SRT and the aeration regime (intermittent aeration). P removal was consistent during Phase 1 (average PO_4^{3-} removal = 83%) excepting aeration failures from reactor control issues around days 80 – 90. Because SRT control was utilized as one of the strategies for NOO out-selection, partial washout of AOO during Phase 1 was occasionally observed when mixed liquor wasting was too aggressive (i.e. total SRT less than 5 days, SRT_{AER} less than 2 days, see Figure S2 and Table 1), resulting in lower NH_4^+ oxidation rates and higher effluent NH_4^+, after which wasting would be suspended to restore AOO mass. The average TIN removal during Phase 1 was 42% but reached >60% during periods of peak performance. The average TSS during Phase 1 was 1,362 ± 623 mg/L, the VSS was 1,052 ± 489 mg/L, and the HRT was 9.7 ± 3.9 hours not including settling and decant.

During Phase 2 (days 247-531), SRT control was optimized (total SRT = 9.2 ± 1.8 days, SRT_{AER} = 3.6 ± 0.9 days) and consistent NH_4^+ and TKN removal (41 ± 24 mgN/L/d and 54 ± 29 mgN/L/d, respectively, considering influent and effluent values with HRT during Period 2) was achieved while maintaining NOO out-selection (described in section 3.1.2). The average HRT of

6.8 ± 2.8 hours (not including settling and decant) was lower than Phase 1 (9.7 ± 3.9 hours) due to improved AOO activity. Average TIN and PO_4^{3-} removal during Phase 2 was 68% and 91%, respectively (Table 2). Biological P removal was not impacted by N removal, and the P uptake rate consistently exceeded the NH_4^+ removal rate during the aerated portion of the cycle (see Figure 2.A&B for PO_4^{3-} and NH_4^+ concentration profiles through typical cycles). This may have contributed to COD limitation for N removal via denitritation, as COD was most depleted at the end of the SBR cycles (Figure 2.A). This in turn may explain NO_2^- accumulation near the end of most cycles and higher P removal than N removal rates. Figure 2.A and 2.B also demonstrates the variability in react length that was often observed throughout the study due to differences in the NH_4^+ oxidation rate, possibly caused by fluctuations in AOO concentrations in the reactor. During Phase 2, the average TSS was 1,773 ± 339 mg/L and the VSS was 1,344 ± 226 mg/L.

3.1.2 NOO Out-selection

A crucial challenge to all shortcut N removal processes, including the nitritation-denitritation with EBPR process that we focus on here, is suppression of NOO activity. To address this challenge, we employed a combination of tight SRT control with intermittent aeration to limit substrate (NO_2^-) accumulation. Process monitoring results demonstrated an elevated nitrite accumulation ratio (NAR) of 70% during Phase 2, suggesting successful suppression of NOO activity (Table 2 and Figure 1). This observation was corroborated by fifteen in-cycle concentration profiles demonstrating NO_2^- accumulation greater than NO_3^- throughout the cycle (see Figure 2.A&B for two representative cycles). In addition, routine maximum activity assays for AOO and NOO demonstrated that during Phase 2 (optimized, stable reactor operation), maximum AOO activity was 3 to 4-fold greater than NOO (Figure 3).

To better understand NOO out-selection and nutrient dynamics during intermittent aeration and to provide additional support for suppression of NOO activity in this process, high frequency sampling (1 grab sample/minute for 40 minutes for measurement of NH_4^+, NO_2^-, NO_3^-, and PO_4^{3-}) was conducted during two typical SBR cycles on days 202 and 258 (Figure 4.A, data from day 258 only shown). The resulting concentration profiles show NO_2^- accumulation with very little NO_3^- accumulation during aeration. Two complete intermittent aeration intervals are shown in the early part of the cycle (note that intermittent aeration begins 45 minutes into the cycle), during which NO_2^- accumulates up to 0.4 mgNO_2^--N/L following 5 minutes of aeration, while NO_3^- does not get above 0.1 mgNO_3-N/L. The NAR during the nitrite peak of these two aeration intervals was 84% and 95%, which demonstrates NOO suppression via selective nitritation. Then, in the subsequent anoxic intervals, the accumulated NO_2^- is drawn down via denitritation. This denitritation provides a robust nitrite sink and one of the methods for NOO out-selection, such that NO_2^- is not available for NOO in the following interval.

Process model results validate the nutrient dynamics observed as seen in Figures 2 and 4, where key state variable profiles from the model match experimental measurements: the average NH_4^+ oxidation and PO_4^- uptake rates, very little NO_3^- accumulation but strong NO_2^- accumulation under aerobic conditions with subsequent drawdown under anoxic conditions, rbCOD consumption in the anaerobic phase, and PO_4^{3-} removal only under aerobic conditions. The process model offers additional insight into the mechanism for NOO out-selection. The net specific growth rates of AOO and NOO were calculated from model data output according to rate equations from the inCTRL ASM matrix (see Supporting Information), and are plotted in parallel with the intermittent aeration intervals in Figure 4.C. Due to differences in substrate availability (i.e. high NH_4^+ and low NO_2^-), μ_{NOO} was less than μ_{AOO} at the beginning of each aeration interval and remained below

359 it throughout the 5 minutes of aeration. This specific growth rate differential was maintained
360 throughout much of the cycle, but μ_{NOO} roughly equaled μ_{AOO} by the end of the intermittently
361 aerated react phase due to the accumulation of NO_2^- (data not shown). However, the differential in
362 net specific growth rates in the early part of the SBR cycle ensures that AOO can be maintained
363 in the reactor at a lower SRT than NOO. The modeled average net specific growth rate (including
364 decay) over the cycle can be used to infer a theoretical SRT for NOO to avoid washout, which in
365 this case was 13.2 days (SRT_{AER} = 5.3 days). A similar calculation using the average net specific
366 growth rate of AOO gives an SRT of 8.2 days (SRT_{AER} = 3.3 days), which affirms that AOO are
367 retained via the modeled SRT of 9.5 days. This differential in theoretical SRT (13.2 days for NOO,
368 8.2 days for AOO) was found with standard kinetic modeling that did not invoke metabolic lag
369 times of NOO (i.e. Gilbert et al., 2014), indicating that substrate limitation alone is sufficient to
370 explain NOO out-competition in this process. The average reactor SRT during Phase 2 was 9.2 ±
371 1.8 days (SRT_{AER} = 3.6 ± 0.9 days) which, because it is in between the theoretical AOO and NOO
372 SRT values indicated above, reinforces experimental data indicating that SRT control was
373 optimized to washout NOO and retain AOO. Both reactor and modeling results therefore confirm
374 that a combination of intermittent aeration and SRT control can be used to maintain nitritation-
375 denitritation under mainstream conditions. Furthermore, these results suggest that NOO
376 suppression via intermittent aeration and SRT control can be explained by simple substrate
377 (kinetic) limitations alone without invoking more complex mechanisms such as metabolic lag time
378 [18] or free ammonia inhibition [19].

379 While intermittent aeration was the primary strategy to suppress NOO activity, the reactor was
380 operated at generally low DO levels between 0 and 1 mgO_2/L. Whether low DO operation itself
381 (aside from the effects of intermittent aeration) confers an advantage to AOO over NOO is unclear.

AOO have historically been thought to have a higher affinity for oxygen than NOO[37], but recent studies have countered that assumption by measuring the opposite, that is, with $K_{O2,NOO} < K_{O2,AOO}$[45,46]. The apparent K_{O2} values measured in those studies were likely affected by floc and microcolony size, which can govern whether AOO or NOO are conferred a competitive advantage at low DO concentrations[47]. In addition, low DO values may promote simultaneous nitritation-denitritation or nitrification-denitrification[48], thus providing a nitrite sink similar to the anoxic periods during intermittent aeration as discussed above. Low peak DO may therefore contribute to NOO suppression based on both competition for O_2 and by promoting nitrite limitation, which supports the argument above that simple kinetics (based only on substrate limitation) can explain NOO out-competition.

3.1.3 N_2O Emissions

N_2O emissions were measured during 8 separate cycles during steady performance in Phase 2 (between days 414 – 531) and ranged from 0.2 to 6.2% of the influent TKN load, with an average of 2.2 ± 2.0% (Table S3). N_2O emissions relative to TIN removal averaged 5.2 ± 4.5%. N_2O accumulation in the reactor generally paralleled NO_2^- accumulation near the end of the aerated portion of the cycle. For example, on the N_2O test on day 414 (Figure 2.B), grab sampling throughout the cycle revealed that by the time NO_2^- first accumulated above 0.1 mgNO_2-N/L at 285 minutes, 57% of the TIN removal for that cycle had occurred while only 20% of the N_2O had been emitted, indicating that relative N_2O emissions increased in the presence of elevated NO_2^-.

The above measurements are comparable to reported N_2O emission rates for conventional biological nutrient removal (BNR) processes. Ahn et al. (2010)[49] reported a range of 0.01 – 1.8% N_2O emitted relative to influent TKN at 12 full-scale wastewater treatment plants (WWTPs),

405 which included both conventional BNR and non-BNR processes. Foley et al., 2010 reported a
406 much larger range of 0.6 – 25% N_2O emitted relative to TIN removed at 7 full-scale conventional
407 BNR WWTPs. See Table 3 for a comparison of N_2O emissions as measured in various treatments
408 processes found in the literature. Both studies found that N_2O emissions were correlated with high
409 NO_2^- concentrations, as was the case in our reactor (Figure 2.B). In fact, of the eight cycles
410 analyzed for N_2O emissions, the four tests with the highest effluent NO_2^- also had the four highest
411 N_2O emissions. Ahn et al. emphasized that the bulk of N_2O emissions occur in aerobic zones due
412 to air stripping of N_2O; indeed, in our reactor 92% of the N_2O emitted from the in-cycle test on
413 day 414 (for example) occurred during aeration. N_2O mass transfer (i.e. stripping) coefficients for
414 our reactor were 40 times higher during aeration and mixing than during mixing alone (0.0688
415 min^{-1} and 0.0017 min^{-1}, respectively). On average, over the course of one cycle 76% of the N_2O
416 production in the reactor was emitted into the gaseous phase while 24% remained in the liquid
417 phase.

418 Other shortcut N removal biotechnologies, such as PN/A, have been found to have elevated
419 N_2O production levels over conventional methods for biological N removal [25–28]. Both Desloover
420 et al.[25] and Kampschreur et al.[28] (who measured 5.1 – 6.6% and 2.3% N_2O production relative to
421 influent TKN, respectively; see Table 3) found that a separate nitritation step (as opposed to
422 simultaneous nitritation and anammox) caused increased N_2O production by AOO, which may be
423 due to elevated NO_2^- concentrations. However, it is not clear that AOO are causing the bulk of
424 N_2O production in our system or other nitritation-denitritation systems, as low COD concentrations
425 can induce incomplete denitrification and lead to elevated N_2O production[51–53]. Low COD
426 conditions (along with low DO) have also been shown to increase N_2O emissions from nitrifier
427 denitrification[54]. Indeed, NO_2^- and N_2O accumulation occurs at the end of the SBR cycles (Figure

2.B) where COD is most depleted from aeration. This suggests that N_2O emissions from this reactor could be mitigated by a step-feed process, i.e. by filling additional primary effluent to prevent a low COD:N ratio and avoid NO_2^- and N_2O accumulation at the end of the cycle. Additional research is required to test the effects of this strategy.

An additional potential benefit of a step-feed modification could be a reduction in the effluent NO_2^- concentration. Elevated NO_2^- concentrations in discharge to surface waters is undesirable in part due to its toxicity to fish and other aquatic life [55]. Aside from a step-feed system, potential solutions to elevated NO_2^- include a final nitrification step (for oxidation of NO_2^- to NO_3^-) or an anammox polishing step (as suggested by Regmi et al., 2015[56]. It should be noted that anammox on seeded biocarriers similar to those in the ANITA^{TM}Mox process[57] could be incorporated into the same reactor for increased N removal, thus eliminating the need for a two-stage system.

3.2 P removal and PAOs

Consistent P removal was achieved in Phase 2 and most of Phase 1 (Figure 1, Table 2). EBPR performance was not negatively impacted by long-term nitritation-denitritation; in fact, the P uptake rate exceeded the NH_4^+ removal rate throughout the study (see Figure 2.A&B for two representative cycles), indicating that SRT and HRT control to optimize AOO activity (while minimizing NOO activity) ensured sufficient retention and react times for PAOs. The total P removal rate during Phase 2 was 6.8 ± 2.7 mgP/L/d when considering the entire SBR cycle. The P uptake rate from in-cycle testing during Phase 2 was 105 ± 34 mgP/L/d (or 3.4 ± 1.1

449 mgP/gVSS/hour) when considering the linear portion of P uptake during the aerated react phase
450 (Figure S3).

451 High frequency sampling (Figure 4.A) and model results (Figure 4.B) both demonstrate P
452 removal during aeration coupled to little to no P removal during periods of anoxia. Importantly,
453 this indicates that P release did not occur in the absence of oxygen, verifying that intermittent
454 aeration with periods of anoxia is compatible with EBPR technologies. However, it also indicates
455 that relatively little denitrifying P uptake occurred, even under anoxic conditions when NO_2^- was
456 present. This suggests that P uptake by aerobic PAO metabolism rather than by denitrifying PAOs
457 (DPAOs) was the predominant driver of P removal. Figure 4.D shows the modeled specific
458 PAO/DPAO growth rates associated with P uptake. Kinetic insights from the process model, which
459 models PAOs as a single group capable of using O_2, NO_2^- and NO_3^- as electron acceptors for P
460 uptake, show that the combination of low NO_2^- and inhibition due to O_2 prevented appreciable
461 DPAO activity during intermittent aeration. Modeled P uptake via NO_2^- was only 16% of total P
462 uptake, and modeled P uptake via NO_3^- was even lower at only 0.7% of total P uptake due to
463 limited NO_3^- accumulation. The process model suggests that the presence of residual DO, rather
464 than a lack of NO_2^- or NO_3^-, was the primary inhibitor of DPAO activity. Figure 4.D shows that
465 peak DPAO growth in the model occurred not at the maximum NO_2^- concentration (i.e. 75
466 minutes) but when DO had reached near zero (i.e. 78 minutes), at which point NO_2^- was at about
467 half of the maximum concentration. Finally, while in-reactor, in-cycle measurements of DPAO
468 activity are difficult to make, *ex situ* measurements of P uptake rates via O_2, NO_2^- and NO_3^- showed
469 that the P uptake via NO_2^- was 17% relative to O_2, while that of NO_3^- was 14% relative to O_2
470 (Figure 5). The high frequency sampling plots, DPAO modeling and *ex situ* P uptake tests all
471 indicate that DPAO activity likely plays a relatively minor role in P removal in this reactor.

The minor role of DPAOs in this process countered our original expectation that frequent periods of anoxia coupled to the presence of NO_2^- would select for a significant DPAO population. DPAOs are considered advantageous in combined N and P removal processes because they offer the opportunity to reduce carbon demand and aeration requirements [58]. Lee et al. (2001) were able to achieve 64% DPAO activity (relative to total P uptake) by introducing a single long anoxic phase (with both NO_2^- and NO_3^- present) in the middle of the aerobic phase, which suggests that longer intermittent aeration intervals may select for more DPAO activity (but perhaps at the expense of NOO out-selection). However, preference for DO does not explain the low P uptake via NO_2^- or NO_3^- in the absence of O_2 (Figure 5) from *ex situ* batch tests in our reactor. Zeng et al. (2003b) observed that *Accumulibacter* PAOs (which were also identified in this study, see Section 3.3) previously acclimated to aerobic P uptake exhibited a 5-hour lag phase in P-uptake when exposed to anoxic conditions (NO_3^-) in place of aeration. A metabolic lag phase is unlikely to explain low maximum P uptake via NO_2^- or NO_3^- in this reactor, however, given that linear drawdown of NO_2^- or NO_3^- was observed in all *ex situ* batch tests. A large majority of *Candidatus* Accumulibacter phosphatis genomes sequenced to date have contained the gene encoding nitrite reductase (responsible for reducing NO_2^- to nitric oxide [NO]) [60], suggesting that most, if not all, *Accumulibacter* PAOs harbor genomic machinery necessary for denitrifying P uptake via NO_2^-. Whether the lack of DPAO activity in this reactor and others is due to the types of PAOs present (and thus the presence or absence of denitrifying genes) or due to the relative expression/inhibition of denitrifying genes present in the PAOs requires further study.

As previously stated, shortcut N removal via nitritation-denitritation did not negatively impact EBPR in this study. Instances of relatively poor P removal were instead usually associated with wet weather flows. Rain not only dilutes the influent but may also induce higher redox conditions

in the collection system, indicating a lack of fermentation and little formation of the VFAs that are beneficial to the EBPR process. On sampling days when primary effluent VFAs were at or below the detection limit of 5 mg acetate/L (n = 21), the average PO_4^{3-} removal of 63% was significantly lower (*p* value = 0.003) than the average PO_4^{3-} removal of 93% on days when VFAs were greater than 5 mg acetate/L (n = 81). For areas with permit requirements below the average of 0.4 ± 0.5 mgTP/L achieved in the reactor effluent, the effects of wet weather flows would need to be mitigated by either occasional exogenous VFA addition or, preferably, primary sludge or return activated sludge fermentation[62]. However, it is commonly considered difficult to achieve < 0.5 mgTP/L with EBPR alone, so for low effluent limits chemical precipitation and/or filtration are often used[63].

Shortcut N removal systems can be problematic for EBPR if NO_2^- accumulation leads to elevated concentrations of its conjugate acid, nitrous acid (HNO_2). HNO_2 concentrations above $0.5x10^{-3}$ mgHNO_2-N/L can lead to inhibition of *Candidatus* Accumulibacter PAOs[64], which were the dominant PAO identified in this study (see Section 3.3). In the extreme case, the maximum NO_2^- concentration in the effluent of our reactor (e.g. end of the SBR cycle) of 5.4 mgNO_2^--N/L combined with the minimum pH of 7.0 (which did not actually occur simultaneously) corresponds to $0.96x10^{-3}$ mg HNO_2-N/L with pK_a of 3.25 for HNO_2 [65]. This indicates that HNO_2 was rarely, if ever, above the reported PAO inhibition concentration in our reactor. Moreover, the highest NO_2^- concentrations occurred near the end of the cycle when the majority of PO_4^{3-} had already accumulated intracellularly as polyphosphate, and residual NO_2^- from the end of the cycle was rapidly depleted after filling at the top of the following cycle.

3.3 Functional Guild Analysis: PAO, NOO, and AOO

We used 16S rRNA gene sequencing to evaluate diversity and relative abundance of PAOs, NOO, and AOO in the reactor. *Candidatus* Accumulibacter was the dominant genus of PAO in the SBR throughout the study and ranged in relative abundance from 6.6% to 12.0% (Figure S4). *Tetrasphaera* was detected at most time points but always below 0.3% relative abundance. Glycogen accumulating organisms (GAOs) in the genus *Candidatus* Competibacter, which are potential competitors to PAOs, were consistently less abundant than PAOs, and varied from below the detection limit to 2.4% relative abundance. Other putative GAOs, such as the genera *Defluviicoccus* and *Propionivibrio* [66], were found at even lower abundance than *Candidatus* Competibacter (data not shown).

Regarding the successful suppression of GAOs in this process, possible influencing factors include SRT, temperature, DO and carbon load. GAOs are thought to effectively compete with PAOs at long SRTs above 20 days[67], which is well above the average SRTs of 11 days (Phase 1) and 9.2 days (Phase 2) of this reactor. PAOs are also known to compete more effectively with GAOs at lower temperatures[68,69], so the moderate temperature of 20 °C utilized in this study may also have assisted GAO suppression. Lower DO concentrations have also been shown to favor PAO activity over GAO activity[70], perhaps due to higher oxygen affinities of PAOs. Finally, the relatively low carbon load in this study (8.2:1 g VFA-COD:g totalP in the influent, and considering the additional demand for carbon for denitritation) may suppress GAO growth. López-Vázquez et al. (2008)[71] found that high influent COD concentrations were positively associated with higher GAO concentrations in full-scale WWTPs, and speculated that the excess carbon (not needed for PAO PHA production) allowed for GAO proliferation.

Nitrotoga and *Nitrospira* alternately dominated the NOO population according to 16S rRNA gene sequencing (Figure 6). The reason for the alternation is unknown as the timing of

succession did not clearly correlate with reactor control or performance, although Keene et al. (2017) observed a similar phenomenon. *Nitrospira* dominated at the beginning of Phase 2, and although the NOO population shifted to *Nitrotoga* over the next 100 – 200 days, there was no corollary change in nitritation-denitritation performance, the NAR, or N removal. This result suggests that the observed robust suppression of NOO activity in this process does not depend upon complete washout of either *Nitrospira* or *Nitrotoga*.

Nitrosomonas-affiliated Betaproteobacteria were the dominant AOO throughout the study according to 16S rRNA gene sequencing but were present at surprisingly low relative abundance for the 2nd half of Phase 1 and all of Phase 2 of reactor operation. Interestingly, the relative abundance of *Nitrosomonas* based on 16S rRNA gene sequencing was below the detection limit for selected samples between days 293 – 431 (Phase 2, Figure 6). No other known AOO were detected during that time; ammonia oxidizing archaea were detected at only two timepoints before day 100 and at low abundance (< 0.04%). Other potential AOO genera, such as *Nitrosospira* and *Nitrosococcus,* were not detected in any 16S rRNA gene sequencing samples. *Nitrospira* can include complete ammonia oxidizing (comammox) clades [73], and comammox can in some cases be the dominant AOO [33] in wastewater treatment. However, *Nitrospira* were not detected or were at low abundance (< 0.04%) after day 293. The decline in AOO was confirmed by qPCR via the functional bacterial *amoA* gene (Figure S5), although AOO were still detected at all time points via qPCR with a minimum of 0.15% relative abundance on day 421. Although the NH_4^+ oxidation rate was variable throughout Phase 2 (Figure S3), NH_4^+ oxidation activity was maintained throughout the experimental period. This suggests that either *Nitrosomonas* AOO can maintain effective NH_4^+ oxidation rates at very low abundance or an as-yet unidentified organism contributed to NH_4^+ oxidation [74].

4. Conclusions

This study is the first to demonstrate robust combined shortcut N and P removal from real wastewater without exogenous carbon or chemical addition at the moderate average wastewater temperature of 20°C. Mainstream nitritation-denitritation was achieved for more than 400 days via intermittent aeration and SRT control, with an average NAR of 70% during Phase 2. Process modeling reproduced this performance and confirmed that NOO activity was suppressed with a combination of NO_2^- drawdown via denitritation and washout via SRT control, and provided possible explanations for the relative lack of DPAO activity. Importantly, neither NO_2^- accumulation nor periods of anoxia in intermittent aeration adversely affected EBPR performance, and consistent and integrated shortcut TIN and biological P removal were achieved for more than 400 days. N_2O emissions were in line with observations of other shortcut N removal systems and were primarily associated with NO_2^- accumulation at the end of the cycle. The single-sludge nutrient removal process examined here, as compared to two-stage systems with separate sludges, could reduce operating cost and complexity while meeting nutrient removal goals. Low DO intermittent aeration as utilized in this study can also reduce aeration demands, thereby reducing electrical costs along with the total carbon footprint of treatment. Moreover, effective removal of limiting nutrients will reduce N and P loads to surface waters, thus potentially reducing the negative effects of eutrophication such as biodiversity loss.

5. Conflicts of Interest

There are no conflicts of interest to declare.

6. Acknowledgements

Many thanks to Christian Landis, Adam Bartecki, George Velez, Sandra Matual, Robert Swanson, Thaís Pluth, Thota Reddy, and O'Brien WRP staff and operators.

This study was funded by the Metropolitan Water Reclamation District of Greater Chicago and the National Science Foundation Graduate Research Fellowship under Grant No. DGE-1324585.

7. References

1 Ll. Corominas, L. Rieger, I. Takács, G. Ekama, H. Hauduc, P. A. Vanrolleghem, A. Oehmen, K. V. Gernaey, M. C. M. van Loosdrecht and Y. Comeau, New framework for standardized notation in wastewater treatment modelling, *Water Sci. Technol.*, 2010, **61**, 841–857.

2 H. Gao, Y. D. Scherson and G. F. Wells, Towards energy neutral wastewater treatment: methodology and state of the art, *Environ. Sci. Process. Impacts*, 2014, **16**, 1223.

3 C. Chan, A. Guisasola and J. A. Baeza, Enhanced Biological Phosphorus Removal at low Sludge Retention Time in view of its integration in A-stage systems, *Water Res.*, 2017, **118**, 217–226.

4 B. Ma, S. Wang, S. Zhang, X. Li, P. Bao and Y. Peng, Achieving nitritation and phosphorus removal in a continuous-flow anaerobic/oxic reactor through bio-augmentation, *Bioresour. Technol.*, 2013, **139**, 375–378.

5 Y. Yang, L. Zhang, H. Shao, S. Zhang, P. Gu and Y. Peng, Enhanced nutrients removal from municipal wastewater through biological phosphorus removal followed by partial nitritation/anammox, *Front. Environ. Sci. Eng.*, , DOI:10.1007/s11783-017-0911-0.

6 M. Zhang, S. Qiao, D. Shao, R. Jin and J. Zhou, Simultaneous nitrogen and phosphorus removal by combined anammox and denitrifying phosphorus removal process, *J. Chem. Technol. Biotechnol.*, 2018, **93**, 94–104.

7 S. Klaus, K. Printz, K. McCullough, V. Srinivasan, D. Wang, P. He, H. De Clippeleir, A. Gu and C. B. Bott, in *Proceedings of the WEF Nutrient Removal and Recovery Symposium*, Water Environment Federation, Minneapolis, MN, USA, 2019.

8 D. S. Lee, C. O. Jeon and J. M. Park, Biological nitrogen removal with enhanced phosphate uptake in a sequencing batch reactor using single sludge system, *Water Res.*, 2001, **35**, 3968–3976.

9 S. Tsuneda, T. Ohno, K. Soejima and A. Hirata, Simultaneous nitrogen and phosphorus removal using denitrifying phosphate-accumulating organisms in a sequencing batch reactor, *Biochem. Eng. J.*, 2006, **27**, 191–196.

10 R. J. Zeng, R. Lemaire, Z. Yuan and J. Keller, Simultaneous nitrification, denitrification, and phosphorus removal in a lab-scale sequencing batch reactor, *Biotechnol. Bioeng.*, 2003, **84**, 170–178.

11 W. Zeng, B. Li, X. Wang, X. Bai and Y. Peng, Integration of denitrifying phosphorus removal via nitrite pathway, simultaneous nitritation–denitritation and anammox treating carbon-limited municipal sewage, *Bioresour. Technol.*, 2014, **172**, 356–364.

12 J. Zhao, X. Wang, X. Li, S. Jia and Y. Peng, Combining partial nitrification and post endogenous denitrification in an EBPR system for deep-level nutrient removal from low carbon/nitrogen (C/N) domestic wastewater, *Chemosphere*, 2018, **210**, 19–28.

13 J. A. Jimenez, G. Wise, G. Burger, W. Du and P. Dold, WEFTEC, New Orleans, LA, 2014.

14 Y. Cao, K. B. Hong, M. C. M. van Loosdrecht, G. T. Daigger, P. H. Yi, Y. L. Wah, C. S. Chye and Y. A. Ghani, Mainstream partial nitritation and anammox in a 200,000 m3/day activated sludge process in Singapore: scale-down by using laboratory fed-batch reactor, *Water Sci. Technol.*, 2016, **74**, 48–56.

15 C. Hellinga, A. A. J. C. Schellen, J. W. Mulder, M. C. M. van Loosdrecht and J. J. Heijnen, The sharon process: An innovative method for nitrogen removal from ammonium-rich waste water, *Water Sci. Technol.*, 1998, **37**, 135–142.

16 J. Zhao, X. Wang, X. Li, S. Jia, Q. Wang and Y. Peng, Improvement of partial nitrification endogenous denitrification and phosphorus removal system: Balancing competition between phosphorus and glycogen accumulating organisms to enhance nitrogen removal without initiating phosphorus removal deterioration, *Bioresour. Technol.*, 2019, **281**, 382–391.

17 B. Ma, P. Bao, Y. Wei, G. Zhu, Z. Yuan and Y. Peng, Suppressing Nitrite-oxidizing Bacteria Growth to Achieve Nitrogen Removal from Domestic Wastewater via Anammox Using Intermittent Aeration with Low Dissolved Oxygen, *Sci. Rep.*, 2015, **5**, 13048.

18 E. M. Gilbert, S. Agrawal, F. Brunner, T. Schwartz, H. Horn and S. Lackner, Response of Different *Nitrospira* Species To Anoxic Periods Depends on Operational DO, *Environ. Sci. Technol.*, 2014, **48**, 2934–2941.

19 Y. Ma, C. Domingo-Félez, B. Gy. Plósz and B. F. Smets, Intermittent Aeration Suppresses Nitrite-Oxidizing Bacteria in Membrane-Aerated Biofilms: A Model-Based Explanation, *Environ. Sci. Technol.*, , DOI:10.1021/acs.est.7b00463.

20 A. C. Anthonisen, R. C. Loehr, T. B. S. Prakasam and E. G. Srinath, Inhibition of Nitrification by Ammonia and Nitrous Acid, *Water Pollut. Control Fed.*, 1976, **48**, 835–852.

21 D. Seuntjens, M. Van Tendeloo, I. Chatzigiannidou, J. M. Carvajal-Arroyo, S. Vandendriessche, S. E. Vlaeminck and N. Boon, Synergistic Exposure of Return-Sludge to Anaerobic Starvation, Sulfide, and Free Ammonia to Suppress Nitrite Oxidizing Bacteria, *Environ. Sci. Technol.*, 2018, **52**, 8725–8732.

22 P. Dold, W. Du, G. Burger and J. Jimenez, Is Nitrite-Shunt Happening in the System? Are Nob Repressed?, *Proc. Water Environ. Fed.*, 2015, **2015**, 1360–1374.

23 N. Hubaux, G. Wells and E. Morgenroth, Impact of coexistence of flocs and biofilm on performance of combined nitritation-anammox granular sludge reactors, *Water Res.*, 2015, **68**, 127–139.

24 M. Laureni, D. G. Weissbrodt, K. Villez, O. Robin, N. de Jonge, A. Rosenthal, G. Wells, J. L. Nielsen, E. Morgenroth and A. Joss, Biomass segregation between biofilm and flocs improves the control of nitrite-oxidizing bacteria in mainstream partial nitritation and anammox processes, *Water Res.*, 2019, **154**, 104–116.

25 J. Desloover, H. De Clippeleir, P. Boeckx, G. Du Laing, J. Colsen, W. Verstraete and S. E. Vlaeminck, Floc-based sequential partial nitritation and anammox at full scale with contrasting N2O emissions, *Water Res.*, 2011, **45**, 2811–2821.

26 C. Domingo-Félez, A. G. Mutlu, M. M. Jensen and B. F. Smets, Aeration Strategies To Mitigate Nitrous Oxide Emissions from Single-Stage Nitritation/Anammox Reactors, *Environ. Sci. Technol.*, 2014, **48**, 8679–8687.

27 A. Joss, D. Salzgeber, J. Eugster, R. König, K. Rottermann, S. Burger, P. Fabijan, S. Leumann, J. Mohn and H. Siegrist, Full-scale nitrogen removal from digester liquid with partial nitritation and anammox in one SBR, *Environ. Sci. Technol.*, 2009, **43**, 5301–5306.

28 M. J. Kampschreur, W. R. L. van der Star, H. A. Wielders, J. W. Mulder, M. S. M. Jetten and M. C. M. van Loosdrecht, Dynamics of nitric oxide and nitrous oxide emission during full-scale reject water treatment, *Water Res.*, 2008, **42**, 812–826.

29 H. Melcer, *Methods for Wastewater Characterization in Activated Sludge Modelling*, IWA Publishing, 2004.

30 D. Mamais, D. Jenkins and P. Prrr, A rapid physical-chemical method for the determination of readily biodegradable soluble COD in municipal wastewater, *Water Res.*, 1993, **27**, 195–197.

31 APHA, *Standard methods for the examination of water and wastewater*, American Public Health Association, Washington, D.C., 21st edn., 2005.

32 M. Laureni, P. Falås, O. Robin, A. Wick, D. G. Weissbrodt, J. L. Nielsen, T. A. Ternes, E. Morgenroth and A. Joss, Mainstream partial nitritation and anammox: Long-term process stability and effluent quality at low temperatures, *Water Res.*, , DOI:10.1016/j.watres.2016.05.005.

33 P. Roots, Y. Wang, A. F. Rosenthal, J. S. Griffin, F. Sabba, M. Petrovich, F. Yang, J. Kozak, H. Zhang and G. F. Wells, Comammox Nitrospira are the dominant ammonia oxidizers in a mainstream low dissolved oxygen nitrification reactor, *Water Res.*

34 O. Schraa, L. Rieger, J. Alex and I. Miletić, Ammonia-based aeration control with optimal SRT control: improved performance and lower energy consumption, *Water Sci. Technol.*, 2019, **79**, 63–72.

35 ifak, 2018.

36 P. S. Barker and P. L. Dold, General model for biological nutrient removal activated-sludge systems: model presentation, *Water Environ. Res.*, 1997, **69**, 969–984.

37 U. Wiesmann, in *Biotechnics/Wastewater*, Springer Berlin Heidelberg, Berlin, Heidelberg, 1994, pp. 113–154.

38 B. Nowka, H. Daims and E. Spieck, Comparison of Oxidation Kinetics of Nitrite-Oxidizing Bacteria: Nitrite Availability as a Key Factor in Niche Differentiation, *Appl. Environ. Microbiol.*, 2015, **81**, 745–753.

39 Y. Law, A. Matysik, X. Chen, S. Swa Thi, T. Q. Ngoc Nguyen, G. Qiu, G. Natarajan, R. B. H. Williams, B.-J. Ni, T. W. Seviour and S. Wuertz, High Dissolved Oxygen Selection against *Nitrospira* Sublineage I in Full-Scale Activated Sludge, *Environ. Sci. Technol.*, 2019, **53**, 8157–8166.

40 H.-D. Park and D. R. Noguera, Characterization of two ammonia-oxidizing bacteria isolated from reactors operated with low dissolved oxygen concentrations, *J. Appl. Microbiol.*, 2007, **102**, 1401–1417.

41 J. S. Griffin and G. F. Wells, Regional synchrony in full-scale activated sludge bioreactors due to deterministic microbial community assembly, *ISME J.*, 2017, **11**, 500–511.

42 A. E. Parada, D. M. Needham and J. A. Fuhrman, Every base matters: assessing small subunit rRNA primers for marine microbiomes with mock communities, time series and global field samples: Primers for marine microbiome studies, *Environ. Microbiol.*, 2016, **18**, 1403–1414.

43 J.-H. Rotthauwe, K.-P. Witzel and W. Liesack, The ammonia monooxygenase structural gene amoA as a functional marker: molecular fine-scale analysis of natural ammonia-oxidizing populations., *Appl. Environ. Microbiol.*, 1997, **63**, 4704–4712.

44 H. Burgmann, S. Jenni, F. Vazquez and K. M. Udert, Regime Shift and Microbial Dynamics in a Sequencing Batch Reactor for Nitrification and Anammox Treatment of Urine, *Appl. Environ. Microbiol.*, 2011, **77**, 5897–5907.

45 P. Regmi, M. W. Miller, B. Holgate, R. Bunce, H. Park, K. Chandran, B. Wett, S. Murthy and C. B. Bott, Control of aeration, aerobic SRT and COD input for mainstream nitritation/denitritation, *Water Res.*, 2014, **57**, 162–171.

46 B. Stinson, S. Murthy, C. Bott, B. Wett, A. Al-Omari, G. Bowden, Y. Mokhyerie and H. De Clippeleir, Roadmap Toward Energy Neutrality & Chemical Optimization at Enhanced Nutrient Removal Facilities, *Proc. Water Environ. Fed.*, 2013, **2013**, 702–731.

47 C. Picioreanu, J. Pérez and M. C. M. van Loosdrecht, Impact of cell cluster size on apparent half-saturation coefficients for oxygen in nitrifying sludge and biofilms, *Water Res.*, 2016, **106**, 371–382.

48 S. M. Hocaoglu, G. Insel, E. U. Cokgor and D. Orhon, Effect of low dissolved oxygen on simultaneous nitrification and denitrification in a membrane bioreactor treating black water, *Bioresour. Technol.*, 2011, **102**, 4333–4340.

49 J. H. Ahn, S. Kim, H. Park, B. Rahm, K. Pagilla and K. Chandran, N2O Emissions from Activated Sludge Processes, 2008−2009: Results of a National Monitoring Survey in the United States, *Environ. Sci. Technol.*, 2010, **44**, 4505–4511.

50 J. Foley, D. de Haas, Z. Yuan and P. Lant, Nitrous oxide generation in full-scale biological nutrient removal wastewater treatment plants, *Water Res.*, 2010, **44**, 831–844.

51 Y.-C. Chung and M.-S. Chung, BNP test to evaluate the influence of C/N ratio on N2O production in biological denitrification, *Water Sci. Technol.*, 2000, **42**, 23–27.

52 Y. Law, L. Ye, Y. Pan and Z. Yuan, Nitrous oxide emissions from wastewater treatment processes, *Philos. Trans. R. Soc. B Biol. Sci.*, 2012, **367**, 1265–1277.

53 F. Sabba, A. Terada, G. Wells, B. F. Smets and R. Nerenberg, Nitrous Oxide Emissions from Biofilm Processes for Wastewater Treatment, *Appl Microbiol Biotechnol*, 2018, 36.

54 N. Wrage, G. L. Velthof, M. L. van Beusichem and O. Oenema, Role of nitrifier denitrification in the production of nitrous oxide, *Soil Biol.*, 2001, 10.

55 W. M. Lewis and D. P. Morris, Toxicity of Nitrite to Fish: A Review, *Trans. Am. Fish. Soc.*, 1986, **115**, 183–195.

56 P. Regmi, B. Holgate, M. W. Miller, H. Park, K. Chandran, B. Wett, S. Murthy and C. B. Bott, Nitrogen polishing in a fully anoxic anammox MBBR treating mainstream nitritation-denitritation effluent: Nitrogen Polishing in a Fully Anoxic Anammox MBBR, *Biotechnol. Bioeng.*, 2015, n/a-n/a.

57 M. Christensson, S. Ekström, A. Andersson Chan, E. Le Vaillant and R. Lemaire, Experience from start-ups of the first ANITA Mox plants, *Water Sci. Technol. J. Int. Assoc. Water Pollut. Res.*, 2013, **67**, 2677–2684.

58 G. Carvalho, P. C. Lemos, A. Oehmen and M. A. M. Reis, Denitrifying phosphorus removal: Linking the process performance with the microbial community structure, *Water Res.*, 2007, **41**, 4383–4396.

59 R. J. Zeng, A. M. Saunders, Z. Yuan, L. L. Blackall and J. Keller, Identification and comparison of aerobic and denitrifying polyphosphate-accumulating organisms, *Biotechnol. Bioeng.*, 2003, **83**, 140–148.

60 P. Y. Camejo, B. O. Oyserman, K. D. McMahon and D. R. Noguera, Integrated Omic Analyses Provide Evidence that a "Candidatus Accumulibacter phosphatis" Strain Performs Denitrification under Microaerobic Conditions, *mSystems*, , DOI:10.1128/mSystems.00193-18.

61 C. M. Sales and P. K. Lee, Resource recovery from wastewater: application of meta-omics to phosphorus and carbon management, *Curr. Opin. Biotechnol.*, 2015, **33**, 260–267.

62 D. S. Skalsky and G. T. Daigger, Wastewater solids fermentation for volatile acid production and enhanced biological phosphorus removal, *Water Environ. Res.*, 1995, **67**, 230–237.

63 K. R. Pagilla, M. Urgun-Demirtas and R. Ramani, Low effluent nutrient technologies for wastewater treatment, *Water Sci. Technol.*, 2006, **53**, 165–172.

64 M. Pijuan, L. Ye and Z. Yuan, Free nitrous acid inhibition on the aerobic metabolism of poly-phosphate accumulating organisms, *Water Res.*, 2010, **44**, 6063–6072.

65 J. R. Rumble, CRC Handbook of Chemistry and Physics 99th Edition, http://hbcponline.com/faces/documents/05_24/05_24_0003.xhtml, (accessed 9 October 2018).

66 M. Stokholm-Bjerregaard, S. J. McIlroy, M. Nierychlo, S. M. Karst, M. Albertsen and P. H. Nielsen, A Critical Assessment of the Microorganisms Proposed to be Important to Enhanced Biological Phosphorus Removal in Full-Scale Wastewater Treatment Systems, *Front. Microbiol.*, , DOI:10.3389/fmicb.2017.00718.

67 J. C. Wang, J. K. Park and L. M. Whang, Comparison of Fatty Acid Composition and Kinetics of Phosphorus-Accumulating Organisms and Glycogen-Accumulating Organisms, *Water Environ. Res.*, 2001, **73**, 704–710.

68 U. G. Erdal, Z. K. Erdal and C. W. Randall, The competition between PAOs (phosphorus accumulating organisms) and GAOs (glycogen accumulating organisms) in EBPR (enhanced biological phosphorus removal) systems at different temperatures and the effects on system performance, *Water Sci. Technol.*, 2003, **47**, 1–8.

69 C. M. Lopez-Vazquez, A. Oehmen, C. M. Hooijmans, D. Brdjanovic, H. J. Gijzen, Z. Yuan and M. C. M. van Loosdrecht, Modeling the PAO–GAO competition: Effects of carbon source, pH and temperature, *Water Res.*, 2009, **43**, 450–462.

70 M. Carvalheira, 2014.

71 C. M. López-Vázquez, C. M. Hooijmans, D. Brdjanovic, H. J. Gijzen and M. C. M. van Loosdrecht, Factors affecting the microbial populations at full-scale enhanced biological phosphorus removal (EBPR) wastewater treatment plants in The Netherlands, *Water Res.*, 2008, **42**, 2349–2360.

72 N. A. Keene, S. R. Reusser, M. J. Scarborough, A. L. Grooms, M. Seib, J. Santo Domingo and D. R. Noguera, Pilot plant demonstration of stable and efficient high rate biological nutrient removal with low dissolved oxygen conditions, *Water Res.*, 2017, **121**, 72–85.

73 H. Daims, E. V. Lebedeva, P. Pjevac, P. Han, C. Herbold, M. Albertsen, N. Jehmlich, M. Palatinszky, J. Vierheilig, A. Bulaev, R. H. Kirkegaard, M. von Bergen, T. Rattei, B. Bendinger, P. H. Nielsen and M. Wagner, Complete nitrification by Nitrospira bacteria, *Nature*, 2015, **528**, 504–509.

74 C. M. Fitzgerald, P. Camejo, J. Z. Oshlag and D. R. Noguera, Ammonia-oxidizing microbial communities in reactors with efficient nitrification at low-dissolved oxygen, *Water Res.*, 2015, **70**, 38–51.

802

803 **Table 1.** SBR cycle timing (gravity fill, anaerobic reactor, aerobic react, wasting, settling, and
804 decant) and reactor control details. The end of the SBR aerobic (intermittently aerated) react
805 phase was determined based on an NH_4^+ setpoint shown in the table.

	Phase 1	*Phase 2*
Days of operation	0 to 246	247 to 531
Gravity fill (min)	3 to 6	
Anaerobic react (min)	45	
Aerobic react via intermittent aeration (min)	317 ± 146	206 ± 105
Wasting (min)	0 to 2.2	
Settling (min)	30 to 40	
Decant of 5/8 volume fraction (min)	4.5 to 6.0	
Online NH_4^+-based control target effluent concentration ($mgNH_4^+$-N/L)	3 to 5	1.5 to 2
Total SRT (days)	11 ± 7	9.2 ± 1.8
Aerobic SRT (days)	4.5 ± 3.0	3.6 ± 0.9
HRT (hours)	9.7 ± 3.9	6.8 ± 2.8

806

807

808 **Table 2.** Arithmetic mean ± standard deviation of composite sampling results for influent
809 (primary effluent) and reactor effluent concentrations. Results from Phase 1 are highlighted in
810 light gray and results from Phase 2 are highlighted in dark gray. Process model predictions are
811 for Phase 2 only. Additional information regarding influent COD fractionation can be found in
812 Table S1.

	Phase 1: Days 0 - 246		*Phase 2: Days 247 - 531*				
	Influent	Reactor Effluent	Influent	Reactor Effluent	Modeled Effluent[a]	Reactor Percent Removal	Modeled Percent Removal[a]
TKN (mgN/L)	21.3 ± 5.1	8.4 ± 4.7	17.9 ± 5.3	2.8 ± 1.2	4.4	85%	76%
NH_4^+ (mgN/L)	15.8 ± 4.2	6.9 ± 4.2	13.5 ± 4.5	1.7 ± 1.1	2.0	87%	85%
NO_2^- (mgN/L)	---[b]	1.5 ± 1.1	---[b]	1.9 ± 1.1	0.3	*not applicable*	
NO_3^- (mgN/L)	---[b]	0.9 ± 1.2	---[b]	0.8 ± 0.5	0.05	*not applicable*	
NAR[c] (%)		62%		70%	85%	*not applicable*	
PO_4^{3-} (mgP/L)	1.8 ± 0.6	0.3 ± 0.4	1.4 ± 0.5	0.1 ± 0.2	0.16	91%	89%
Total P (mgP/L)	2.6 ± 0.6	0.4 ± 0.5	2.2 ± 0.7	0.4 ± 0.5	1.0	83%	56%
Total COD (mgCOD/L)	176 ± 55	30 ± 24	150 ± 46	28 ± 11	47	81%	69%
Filtered COD[d] (mgCOD/L)	107 ± 31	27 ± 17	94 ± 32	24 ± 6	27	74%	72%
Alkalinity (meq/L)	4.6 ± 0.9	3.8 ± 0.7	4.7 ± 0.6	3.8 ± 0.7	4.1	20%	13%
TSS (mg/L)	50 ± 27	12 ± 28	72 ± 47	18 ± 19	23	75%	68%

[a] *Average primary effluent values from Phase 2 were used as influent to the process model*

[b] *79% of influent NO_x^- (combined NO_2^- + NO_3^-) measurements below the detection limit of 0.15 mgN/L*

[c] *NAR = nitrite accumulation ratio*

[d] *"Filtered COD" indicates filtration through 1.2 μm filter, not to be confused with "floc-filtered COD" (see Methods)*

813

814

Table 3. Summary of N_2O emission measurements reported in the literature for conventional and shortcut N removal processes. Conventional nitrogen removal processes (nitrification-denitrification) are highlighted in grey while shortcut nitrogen removal processes (nitritation-denitritation and nitritation-anammox) are highlighted in white.

	Nitrogen removal method	Reactor configuration	N_2O Emissions (%N_2O-N / TKN load)	N_2O Emissions (%N_2O-N / N removed)	Reference
Conventional	Nitrification-denitrification or none	12 full-scale WWTPs (BNR & non-BNR)	0.01 to 1.8	0.01 to 3.3	Ahn et al. (2010)
	Nitrification-denitrification	7 full-scale BNR WWTPs	---	0.6 to 25	Foley et al. (2010)
	Denitrification (varying C:N ratios)	1 lab-scale semi-continuous	0.005 to 0.5	---	Chung and Chung (2000)
Shortcut Nitrogen	Nitritation-anammox (two stage)	1 full-scale 4-stage "New Activated Sludge"	5.1 to 6.6	---	Desloover et al. (2011)
	Nitritation-anammox (two stage)	1 full-scale process	2.3	---	Kampschreur et al. (2008)
	Nitritation-anammox (single stage)	2 lab-scale SBRs	---	1.7 to 10.9	Domingo-Feléz et al. (2014)
	Nitritation-denitritation	1 lab-scale SBR	2.2 ± 2.0	5.2 ± 4.5	*This study*

Definitions: BNR = Biological nutrient removal, WWTP = wastewater treatment plant, SBR = sequencing batch reactor

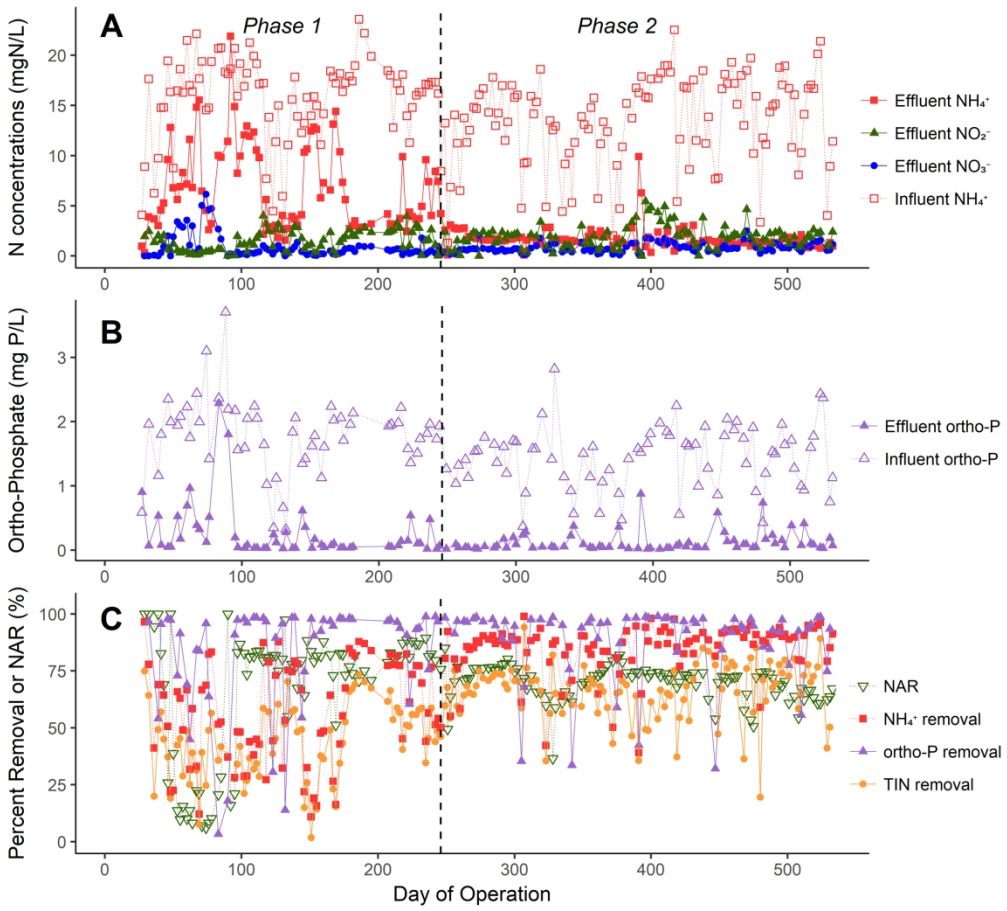

Figure 1. Reactor performance over time from composite sampling (2 – 3 samples/week) over the entire study. A) Influent (primary effluent) NH_4^+ and effluent NH_4^+, NO_2^-, and NO_3^-. B) Influent and effluent orthophosphate. C) Nitrite accumulation ratio (NAR) and percent removal of NH_4^+, orthophosphate and TIN.

186x169mm (300 x 300 DPI)

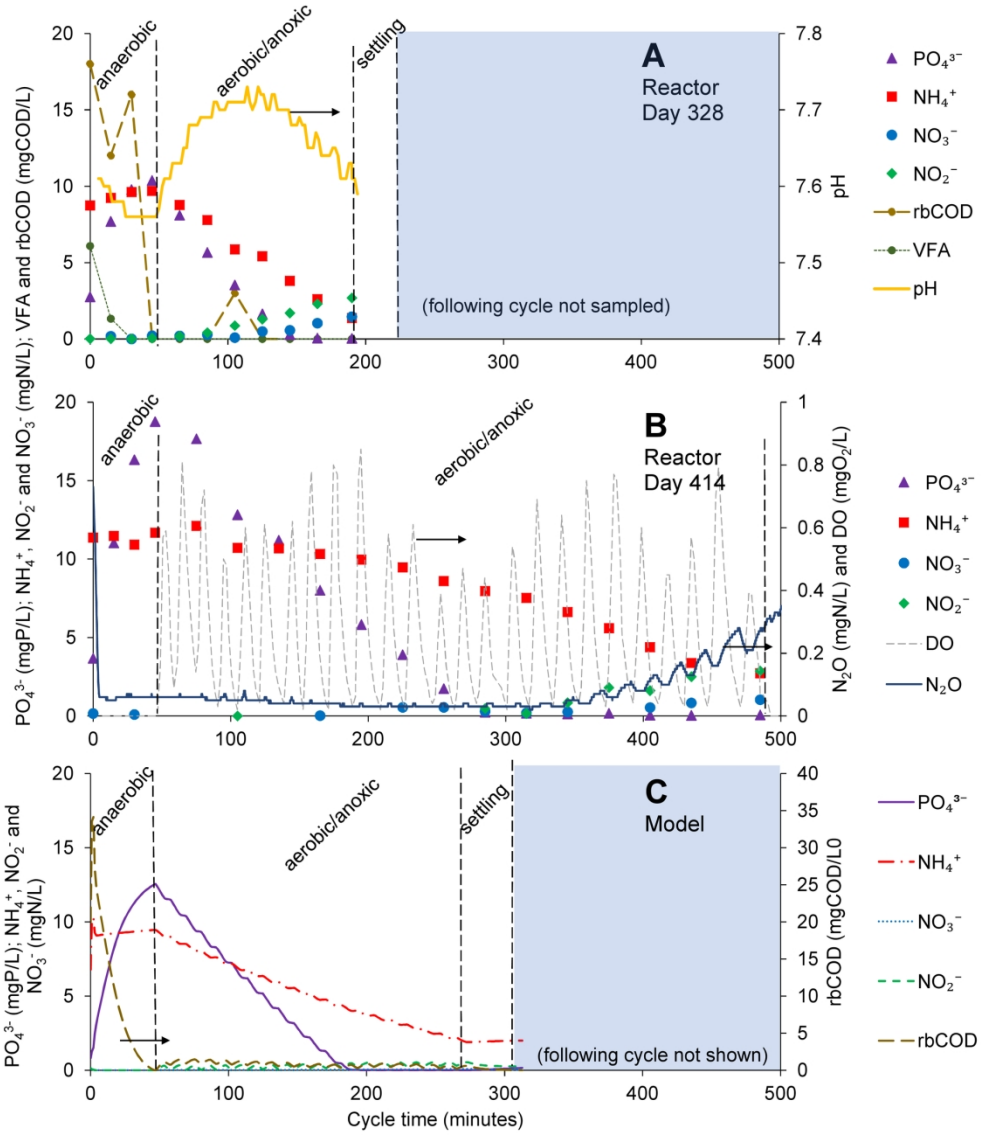

Figure 2. A) and B) Two react cycles on days 328 and 414, respectively, that demonstrate efficient P and N removal, selective nitritation, and variability in aerated react length. Cycle A included measurements for rbCOD and VFAs, and cycle B was run with an N2O sensor in the reactor. C) SBR cycle as modeled in SIMBA#. rbCOD as shown was calculated as soluble COD_t – soluble $COD_{effluent}$.

173x200mm (300 x 300 DPI)

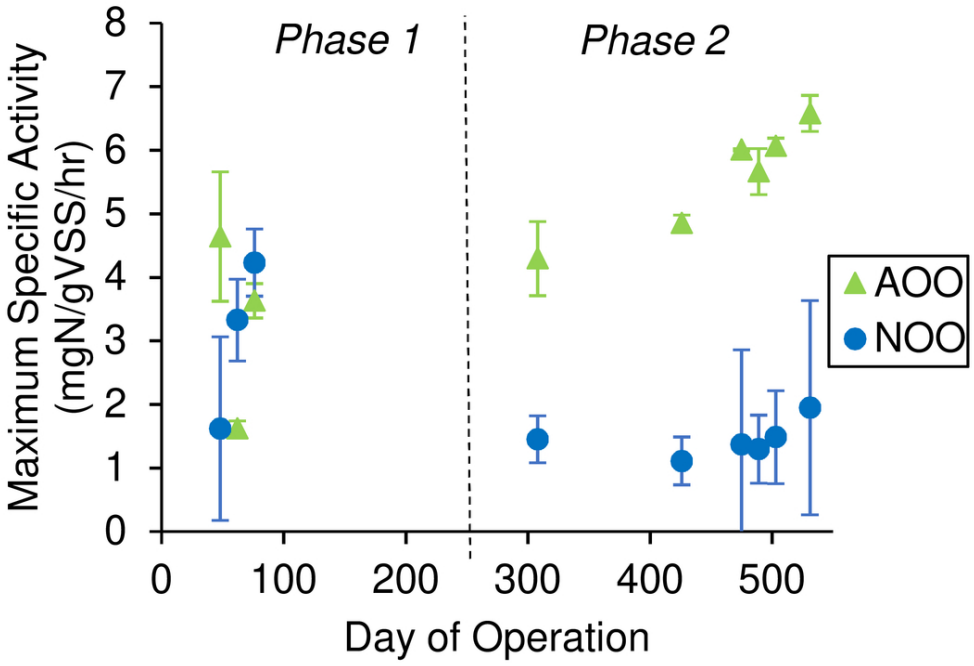

Figure 3. Maximum specific AOO and NOO activity as measured by *ex situ* batch testing. Error bars represent the standard deviation of the method replicates.

91x64mm (300 x 300 DPI)

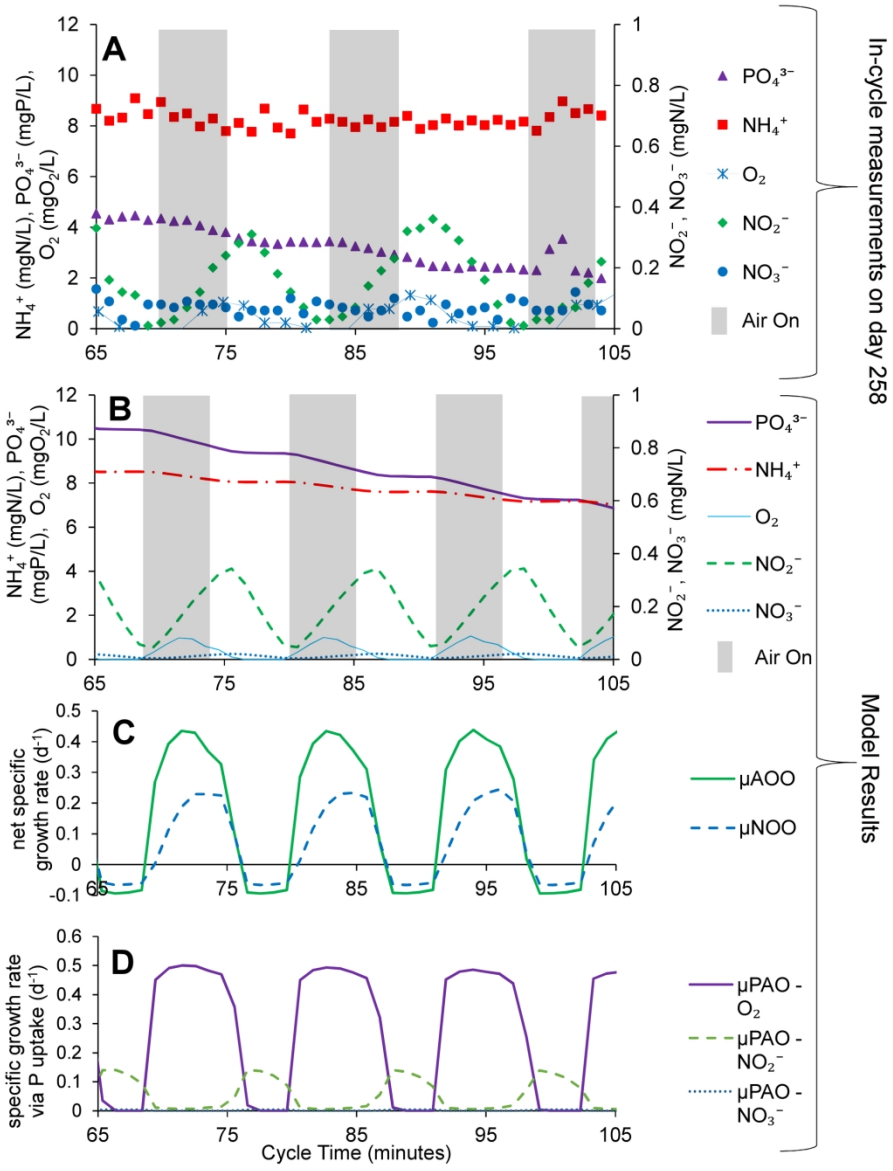

Figure 4. Comparison plot between high resolution within-cycle reactor sampling (A) and modeled results (B, C, D) for the intermittently aerated react period of SBR operation (minutes 65 – 105, beginning 20 minutes after the start of aeration). A) Results of grab sampling from a reactor cycle on day 258 of operation. Selective nitritation rather than nitratation during aerated phases (gray shading) is evident and produced NO_2^- is then denitrified in anoxic phases. The s::can optical DO sensor is rated for a 60-second response time, and a ~1-minute delay is evident in comparison to the model plot B. B) Modeled concentration dynamics including on/off switching for aeration control. C) Modeled AOO and NOO net specific growth rates including decay. D) Modeled PAO specific growth rates associated with P uptake via O_2, NO_2^- and NO_3^-. Decay and growth not associated with P uptake are not included.

176x230mm (300 x 300 DPI)

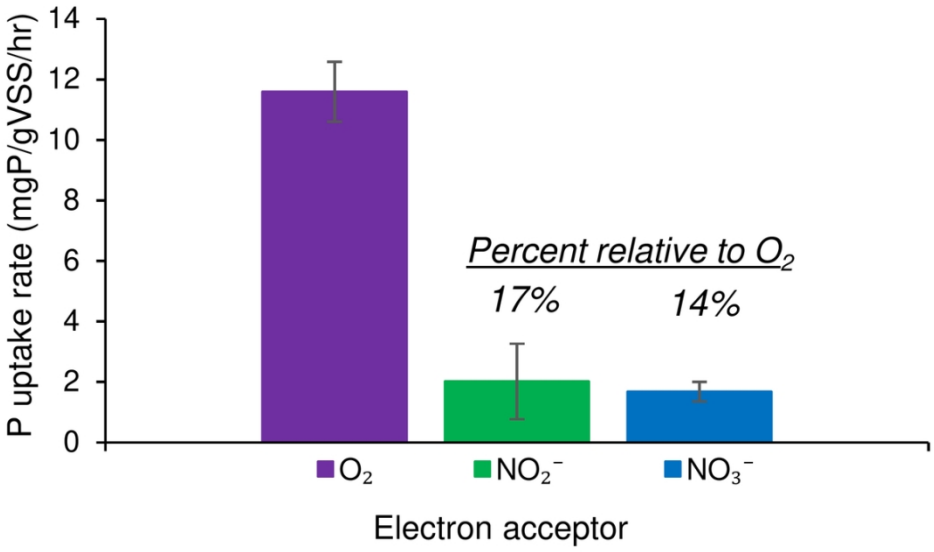

Figure 5. P uptake rates in the presence of O_2, NO_2^-, and NO_3^- from *ex situ* batch tests.

107x64mm (300 x 300 DPI)

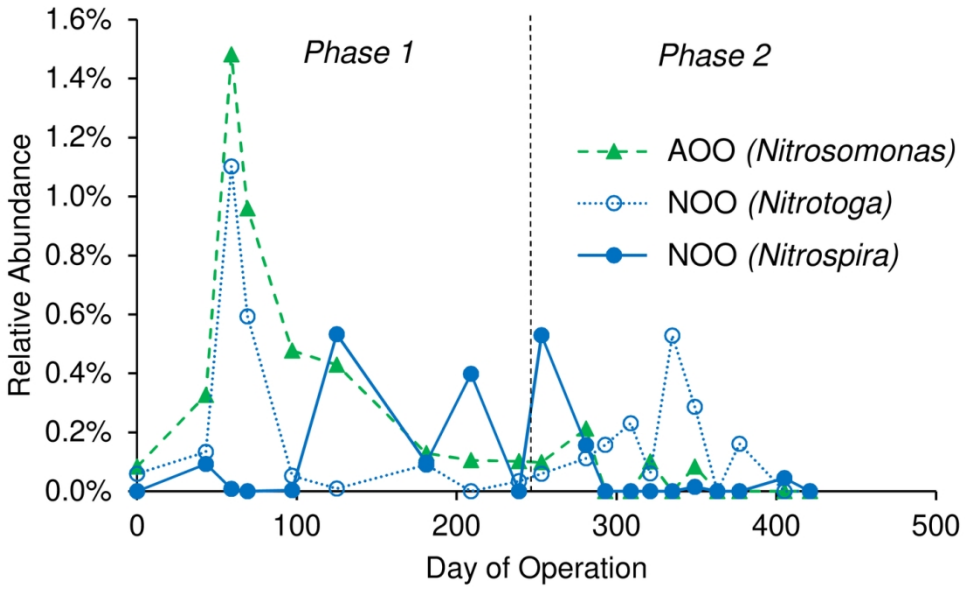

Figure 6. Relative AOO and NOO abundance based on 16S rRNA gene amplicon sequencing through the first 421 days of reactor operation. Day "0" represents the inoculum, which was sampled before reactor operation began.

126x79mm (300 x 300 DPI)

Summary graphic:

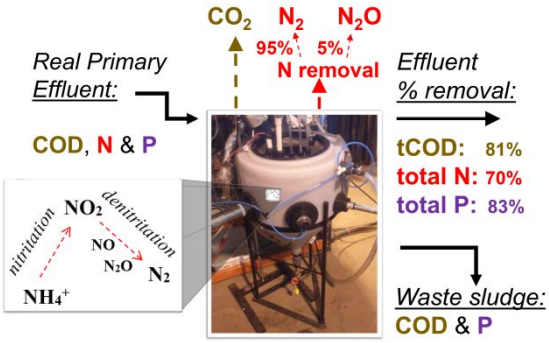

Summary sentence: Combined nitritation-denitritation and biological phosphorus removal from real wastewater was achieved for more than 400 days without chemical addition.